Article:
Dhimish, Mahmoud, Theristis, Marios and d'Alessandro, Vincenzo (2024) Photovoltaic hotspots: a mitigation technique and its thermal cycle. Optik. 171627. ISSN: 0030-4026

https://doi.org/10.1016/j.ijleo.2024.171627

Photovoltaic hotspots: a mitigation technique and its thermal cycle

Mahmoud Dhimish[1]*, Marios Theristis[2], Vincenzo d'Alessandro[3]

[1] School of Physics, Engineering and Technology, University of York, York YO10 5DD, United Kingdom

[2] Sandia National Laboratories, Albuquerque, NM 87185 USA

[3] Department of Electrical Engineering and Information Technologies, University of Naples Federico II, Napoli, 80138 Napoli NA, Italy

*Corresponding Author, M. Dhimish (Mahmoud.dhimish@york.ac.uk)

Abstract

In the rapidly evolving field of solar energy, Photovoltaic (PV) manufacturers are constantly challenged by the degradation of PV modules due to localized overheating, commonly known as hotspots. This issue not only reduce the efficiency of solar panels but, in severe cases, can lead to irreversible damage, malfunctioning, and even fire hazards. Addressing this critical challenge, our research introduces an innovative electronic device designed to effectively mitigate PV hotspots. This pioneering solution consists of a novel combination of a current comparator and a current mirror circuit. These components are uniquely integrated with an automatic switching mechanism, notably eliminating the need for traditional bypass diodes. We rigorously tested and validated this device on PV modules exhibiting both adjacent and non-adjacent hotspots. Our findings are groundbreaking: the hotspot temperatures were significantly reduced from a dangerous 55°C to a safer 35°C. Moreover, this intervention remarkably enhanced the output power of the modules by up to 5.3%. This research not only contributes a practical solution to a longstanding problem in solar panel efficiency but also opens new pathways for enhancing the safety and longevity of solar PV systems.

Keywords: Photovoltaics; solar cells; hotspots; cracks; performance analysis; power electronics.

---

1. Introduction

As the integration of photovoltaic (PV) systems into the energy grid accelerates, driven by the imperative for renewable energy expansion, the reliability and longevity of these systems have captured significant industry focus. The prevalence of mismatch conditions in PV installations, leading to inefficiencies in energy production, has been widely documented [1-3]. Among the most critical of these inefficiencies are the thermal anomalies known as hotspots. These hotspots represent zones of elevated temperature localized within specific areas of a PV module, which can cause substantial increases in the temperature of solar cells, consequently impacting the module's overall performance. Fig. 1 [5] vividly illustrates this condition, displaying a PV module in operation with four cells experiencing an intense localized temperature peak of 56.1°C. The thermal image captures the stark contrast between the hotspots and the surrounding cells, underscoring the urgency for effective diagnostic and mitigation strategies in the field.

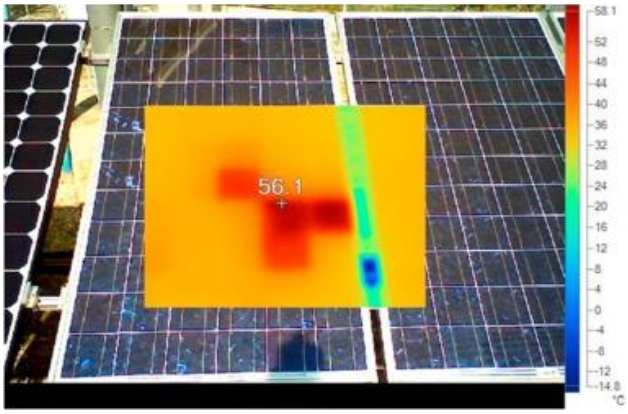

Fig. 1. Example of a PV module that is affected by multiple hotspots [5].

Research into the causation and underlying mechanisms of hotspots in PV modules is ongoing. Current studies indicate that hotspots may arise due to drastic diurnal temperature swings, which are especially pronounced in regions like deserts and coastal areas [6, 7]. Dhimish *et al.* [7] noted that a single hotspot string could precipitate a substantial 25% reduction in a PV module's power output and potentially trigger a temperature surge of up to 65°C. It is important to note that in their analysis, the PV sub-strings were assessed indoors under Standard Test Conditions (STC), providing a controlled baseline for evaluating performance. Further investigations have linked the occurrence of PV hotspots to physical imperfections, such as micro-cracks within solar cells [8, 9]. These defects are not merely a thermal hazard but can also considerably diminish the electrical output of PV modules. In severe instances, the resulting thermal stress may even compromise the integrity of bypass diodes [10, 11].

Conventionally, thermal imaging cameras have been the tool of choice for identifying hotspots due to their ability to visually capture temperature anomalies [12, 13]. Advancing beyond visual techniques, recent research has explored the application of machine learning algorithms capable of detecting hotspots through the analysis of electrical performance metrics, including output voltage, current, and dynamic series resistance [14, 15]. These innovative approaches promise to enhance the precision and early detection of hotspots, potentially mitigating their adverse effects on PV module performance.

While the methods previously discussed are primarily concerned with field diagnostics, hence offering a reactive means to detect hotspots, proactive mitigation techniques are comparatively less developed. Among the progressive strategies, the use of dual metal-oxide-semiconductor field-effect transistors (MOSFETs) have been noteworthy. This approach involves deploying two MOSFETs with the PV module—one arranged in series and the other in parallel, as exemplified in Fig. 2(a) [16-18]. The MOSFETs function as switches that regulate current flow passively, alternating between ON and OFF states at a high frequency to modulate the delivery of current from the PV module. This technique helps to prevent the formation of hotspots by ensuring a balanced distribution of current across the module.

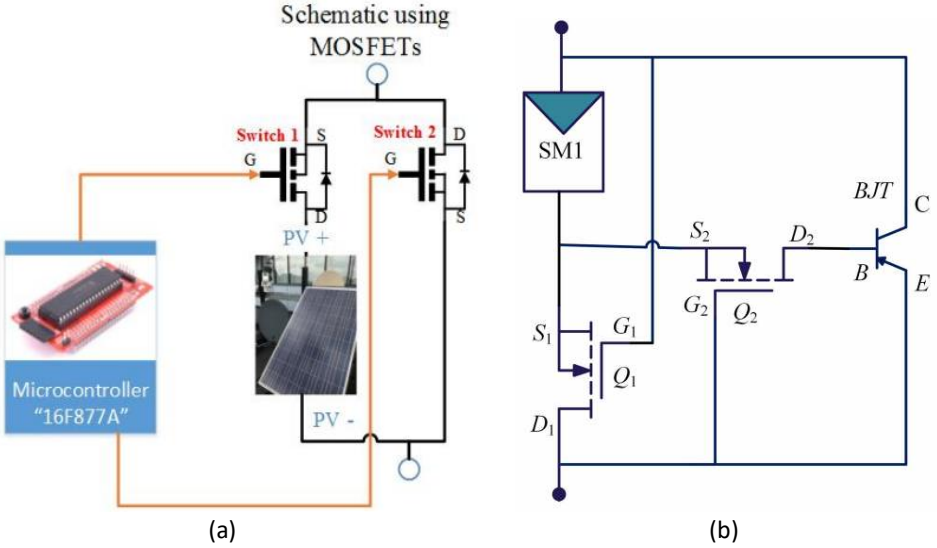

Fig. 2. PV hotspot mitigating techniques, (a) Dual MOSFET concept [16], (b) BJT-Based bypass concept [19].

An alternative design, illustrated in Fig. 2(b), involves a bipolar junction transistor (BJT)-based bypass system, initially introduced by d'Alessandro *et al. [*19]. This system employs a pair of MOSFETs that dynamically regulate the BJT's operation, enabling or inhibiting its conduction in response to changing conditions. Additionally, the inclusion of an antiparallel Schottky diode provides supplementary support to the BJT, particularly under conditions of critical shading, enhancing the protection against hotspots.

However, the practicality of this BJT-based approach is limited by certain drawbacks. The necessity for continual switching, intrinsic to this design, introduces complexity. Moreover, its integration within the PV sub-strings poses challenges, as it complicates the circuit and increases costs, which may not be feasible for deployment in large-scale PV systems where simplicity and cost efficiency are paramount.

Recent advances in PV system technology have continued to address the persistent challenge of hotspots, which significantly affect module reliability and output performance. A notable contribution to the field is the work of Tang *et al.* (2019) [20], which provides a thorough review of current hotspot mitigation strategies. Their research offers a comprehensive comparison of these strategies by examining mitigating costs, power loss, hotspot temperature, and the overall output power of PV panels. Furthermore, they have innovatively developed an intuitive evaluation method based on area assessment, allowing for a more straightforward comparison of the efficacy of different hotspot mitigation approaches. This

method serves as a valuable tool for researchers and industry professionals seeking to assess and implement cost-effective and efficient hotspot mitigation solutions.

Another significant development in hotspot mitigation is the novel circuit proposed by Ghosh *et al.* (2020) [21]. This circuit, referred to as the Hot Spot Mitigation Circuit (HSMC), is designed to effectively reduce cell temperature under mismatch conditions through a modified bypass approach. By focusing on thermal regulation without the need for regular switching mechanisms, this circuit aims to enhance the reliability of PV modules. The introduction of such a technique represents a step forward in simplifying the mitigation process, potentially reducing the complexity and cost associated with large-scale PV system maintenance.

Additionally, a recent study [22] has introduced a groundbreaking approach to mitigate the effects of partial shading, a common precursor to hotspot formation in PV modules. Their strategy revolves around preventing the activation of bypass diodes, thus reducing the incidence of hotspots in mismatched cells. They also advocate for a split submodules approach, which is suggested as a simpler and potentially more scalable solution for widespread PV system applications. This innovative approach underscores the shift towards more adaptable and programmable PV subsystems, aligning with the industry's move towards more intelligent and responsive energy systems.

In this work, we introduce an innovative circuit designed for the mitigation of hotspots in PV modules. Our solution sets itself apart by eschewing traditional bypass diodes, thus avoiding their associated limitations, and instead employs an automatic switching mechanism that ensures dynamic response to fluctuating thermal conditions. The circuit we propose is distinguished by its simplicity and efficacy, comprising two pivotal stages: the first is a current comparator that detects anomalies in the current flow indicative of potential hotspots, and the second is a current mirror circuit that responds to these anomalies by adjusting the current flow, thereby mitigating the hotspot. This design allows for precise control of the input and output current via a purely resistive element, promoting a more stable and efficient operational environment for the PV module.

The structure of this paper is crafted to guide the reader through our methodology and findings systematically. In Section 2, we delve into the specifics of our proposed mitigation technique, elaborating on the nuances of the hardware implementation that enable its functionality. Section 3 is dedicated to the empirical validation of our technique, presenting two distinct case studies: one involving a PV module affected by adjacent hotspots and the other by non-adjacent hotspots. These case studies demonstrate the versatility and robustness of our approach under different challenging conditions. Finally, Section 4 synthesizes our findings into a cohesive conclusion, encapsulating the implications and potential impact of our research on the field of PV system reliability and efficiency.

2. Proposed Mitigation Technique

Section 2 details the development and architecture of an electronic circuit specifically designed for integration with PV modules to mitigate the effects of hotspots. The heart of this system lies in its simplicity and functionality, as depicted in Fig. 3(a), which illustrates the actual circuit design. Fig. 3(b) delineates the physical connections of ports 1, 2, and 3, which are crucial for the operation of the circuit. To alleviate any confusion, it should be noted that the circuit is indeed designed for application across PV modules, which comprise strings of PV cells. This distinction is crucial for understanding the scalability and application of the mitigation strategy.

Before delving into the circuit design, it is essential to establish the fundamental principles that underpin our method. Hotspot mitigation in PV modules is predicated on the need to balance current flow across the module to prevent the excessive heat buildup that characterizes hotspots. This balance is achieved by detecting and responding to variations in current that indicate potential overheating. Our method is grounded in the principle that a uniform current across a PV module's cells or strings can prevent the temperature spikes leading to efficiency loss and material degradation.

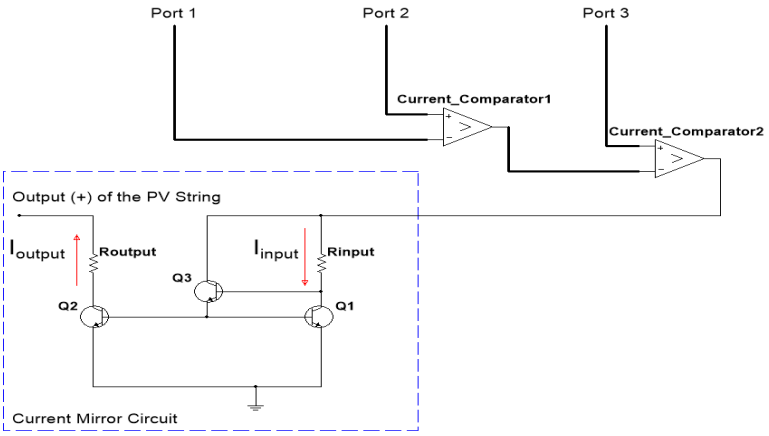

(a)

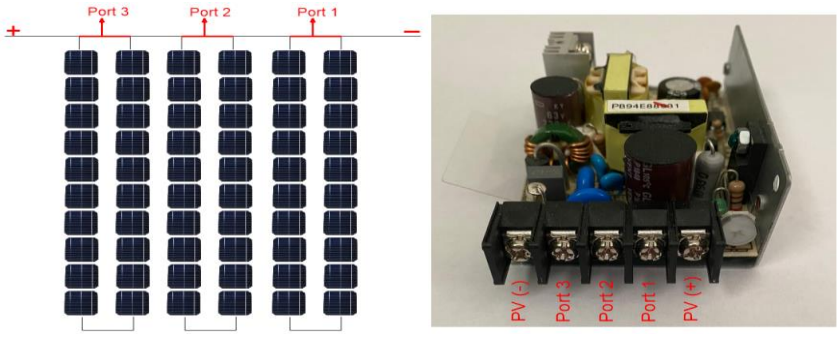

(b)

Fig. 3. (a) Proposed electronic circuit for PV hotspots mitigation, (b) Physical connection of ports 1-3 and the hardware circuit design, the circuit also has a buck dc-dc converter for use with maximum power point tracking, if required to be used.

In the proposed method, our circuit employs a dual-stage current comparator setup. The first stage utilizes the current comparator to measure and compare the output currents from the first and second PV sub-strings, accessed through ports 1 and 2, respectively. The differential current obtained from this comparison is then juxtaposed with the current from the last PV sub-string, connected through port 3. This step is critical as it ensures that the current across all sub-strings is balanced, preventing the occurrence of hotspots.

Subsequently, the harmonized current flows into the current mirror circuit, which serves a dual purpose. Primarily, it maintains equilibrium between the output current and the maximum permissible current at the load end. Additionally, it functions as a regulatory mechanism, ensuring the current is within the optimal range for efficient energy production. The current at the base of transistor Q3 is governed by (1) and (2).

$$I_{E3} = I_{B1} + I_{B2} = I_E \left(\frac{2}{1+\beta}\right) \tag{1}$$

$$I_{B3} = I_{E3} \left(\frac{1}{1+\beta}\right) = I_E \left(\frac{2}{1+\beta}\right)\left(\frac{1}{1+\beta}\right) = \frac{2\ I_E}{(1+\beta)^2} \tag{2}$$

Here, I_E represents the emitter current in the transistor, and β denotes the gain or amplification factor of the transistor; I_{B1}, I_{B2}, and I_{B3} are Base currents in the transistors Q1, Q2, and Q3, respectively, which are the controlling currents for the transistor operation; I_{C1} and I_{C2} are Collector currents in the transistors Q1 and Q2, respectively, representing the current flowing through the collector terminal. The value of β is typically found in the transistor's datasheet, with a common range between 50 to 350. Equations (3) and (4) facilitate the computation of the input and output currents:

$$I_{input} = I_{C1} + I_{B3} = \frac{I_E\,\beta}{(1+\beta)} + \frac{2\ I_E}{(1+\beta)^2} = I_E \left(\frac{2+\beta(1+\beta)}{(1+\beta)^2}\right) \tag{3}$$

$$I_{output} = I_{C2} = \frac{I_E\,\beta}{1+\beta} \tag{4}$$

The effectiveness of the current mirror circuit is quantified by the gain ratio of the output to input current, as expressed in (5). Subsequently, (6) predicts the final output current from the PV module, which is a function of the input current and a factor solely dependent on the β value of the transistor.

$$\frac{I_{output}}{I_{input}} = \frac{1}{1+\frac{2}{\beta^2+\beta}} \tag{5}$$

$$I_{output} = I_{input} \left(\frac{1}{1+\frac{2}{\beta^2+\beta}}\right) \tag{6}$$

To tailor the input and output current to specific needs, resistors R_{input} and R_{output} are strategically placed within the current mirror circuit, which are typically the input and output resistors connected to the mirror circuit. This arrangement affords the flexibility to modulate the current by adjusting the resistance values, thereby optimizing the circuit's performance under various operating conditions. Importantly, the inclusion of these resistive elements does not detract from the circuit's efficiency; they operate passively and engender minimal power losses.

3. Results

In this section, the evaluation of the proposed hotspots mitigation circuit design is presented. The section comprises of two case studies including: the PV module affected by adjacent hotspots and another PV module affected by non-adjacent hotspots. All the obtained results were taken while operating the PV modules at STC conditions, where the solar irradiance is equal to 1000 W/m^2, and cell temperature is 25°C. The electrical characteristics of the evaluated PV modules, when measured under STC, are as follows: the maximum power output ($Pmax$) is 220 watts, the open-circuit voltage (Voc) is 28.7 volts, and the short-circuit current (Isc) is 8.17 amperes.

3.1 PV Module Affected by Adjacent Hotspots

The thermal characteristics of the first examined PV module are visually represented in Fig. 4. This thermal image was obtained using a FLIR i7 infrared camera, which is well-regarded for its precision in thermal detection. The FLIR i7 is equipped with a focal plane array sensor that provides a resolution of 140 x 140 pixels, allowing for detailed thermal mapping. It operates within the spectral range of 7.5 to 13 µm, which is optimal for detecting thermal anomalies in PV modules. With a thermal sensitivity of ±0.1°C, the camera can accurately identify minute temperature variations, critical for pinpointing potential hotspots. In the captured image, three adjacent anomalies are discernible, each exhibiting a significant temperature increase. These hotspots register an approximate temperature of ~50°C, which starkly contrasts with the surrounding healthy solar cells that maintain a temperature near 25°C. The FLIR i7 camera's ability to detect such fine thermal differences is instrumental in the assessment of PV module health and the effectiveness of our hotspot mitigation techniques.

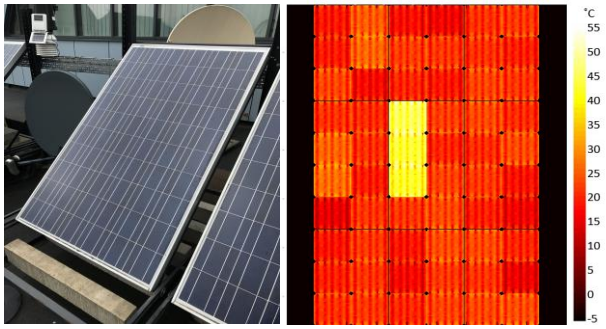

Fig. 4. Physical and thermal image of the first examined PV module affected by adjacent hotspots.

The PV module shown in Fig. 4, once interfaced with the proposed mitigation circuit, underwent a thermal monitoring cycle with intervals of one minute, extending over a period of ten minutes. Sequential thermal imagery captured during this duration is illustrated in Fig. 5. Initially, the hotspots presented as areas of pronounced localized heat, exhibiting temperatures significantly higher than those of the unaffected solar cells. Over time, a marked reduction in the temperature of these hotspots was observed. Notably, by the end of the fourth minute, the temperature of the hotspot-afflicted cells had converged towards equilibrium with the healthy cells. This thermal transition plateaued thereafter, indicating the achievement of a steady state. The experiment thus substantiates the efficiency of the circuit, demonstrating that a mere four minutes is sufficient for the mitigation circuit to ameliorate the hotspot condition and stabilize the temperature across the module.

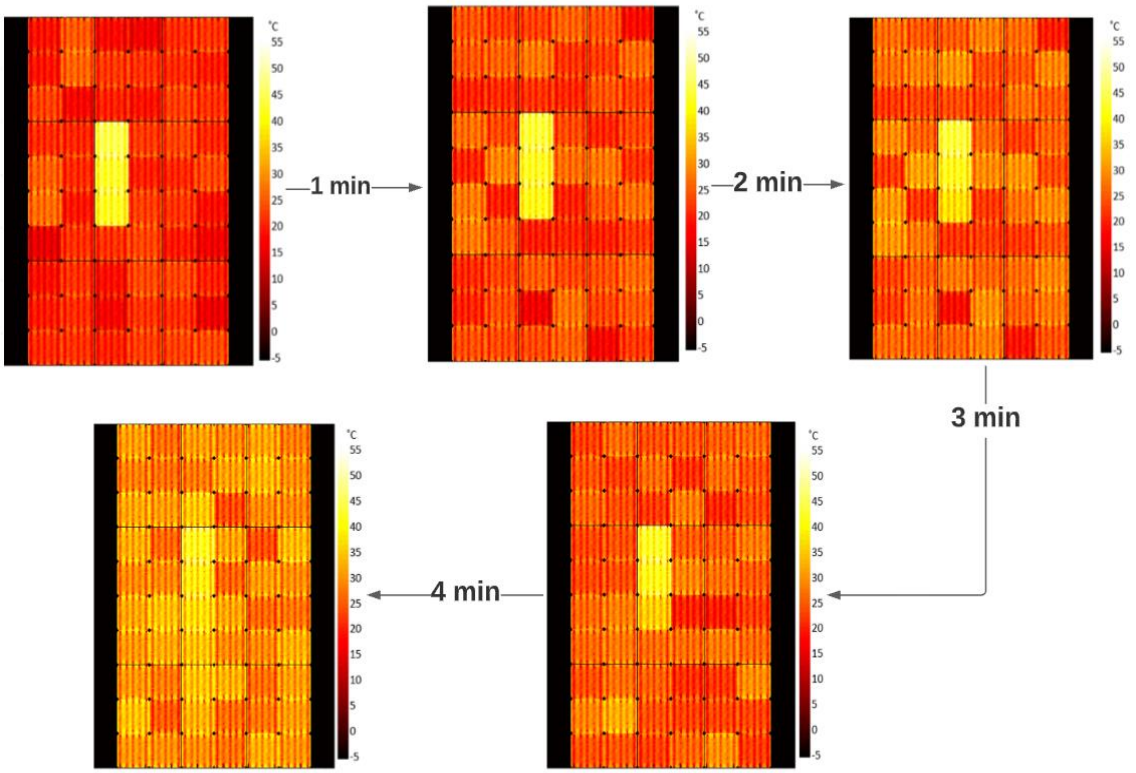

Fig. 5. Thermal cycle of the PV module affected by adjacent hotspots after using the proposed circuit design.

Table 1 provides a time-resolved thermal analysis of PV module hotspots after the implementation of the mitigation circuit. At the initial stage (1 minute), the hotspots exhibit a significant temperature differential, registering an average of 50°C, which is notably higher than the 25°C observed in the surrounding healthy cells. As time progresses, the efficiency of the mitigation circuit becomes evident. After 2 minutes, the average temperature of the hotspots decreases to 45°C, and this downward trend continues, with the hotspots further cooling to an average of 40°C at the 3-minute mark. By the 4-minute interval, the hotspots have substantially cooled to an average temperature of 32°C, approaching the baseline temperature of the surrounding cells, which have concurrently warmed slightly to 28°C. This demonstrates not only the effectiveness of the mitigation circuit in reducing hotspot temperatures but also its rapid action, as a near equilibrium state is achieved within 4 minutes of circuit operation.

Table 1. Time-Resolved Thermal Analysis of PV Module (shown in Fig. 5) Hotspots Post Mitigation Circuit Implementation.

Time (min)	Average Temperature of Hotspots (°C)	Average Temperature of Surrounding Cells (°C)	Notes
1	50	25	Initial thermal image showing distinct hotspots.
2	45	25	Slight decrease in hotspot temperature.
3	40	26	Continued decrease towards healthy cell temperature.
4	32	28	Hotspot temperature nearly matches healthy cells.

In the optimized circuit configuration, heat distribution across the PV module surface is actively managed by controlling the output current from each sub-string. Fig. 6(a) illustrates the operational currents where the first sub-string delivers 7.77 A, and the subsequent sub-strings provide 7.17 A and 7.73 A, respectively. The current comparators play a pivotal role in this regulation, with the first comparator outputting 7.73 A—this being the higher current compared to the 7.17 A from the second sub-string. A marginal current reduction is observed in the output from the second current comparator, which provides 7.74 A. This slight drop to 7.74 A is attributed to the inherent voltage drop across the comparator; it's noteworthy that such a drop is not present after the first comparator because it outputs the current from the first sub-string directly without encountering the voltage drop that is typically associated with comparator operation.

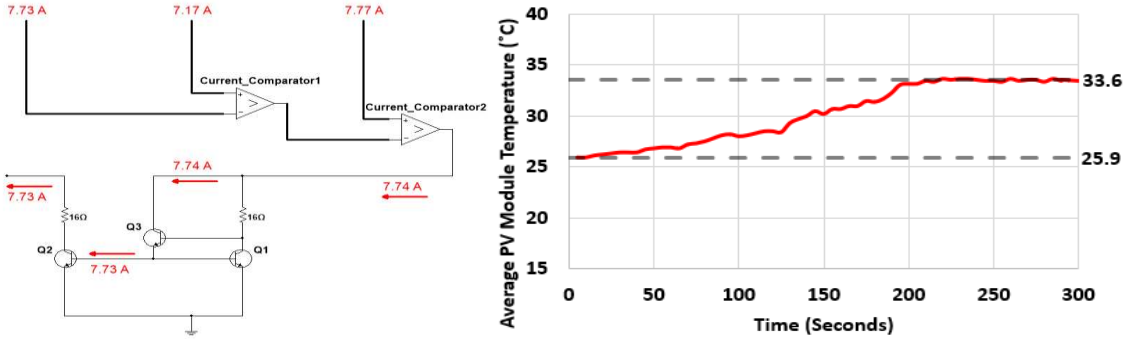

(a) (b)

Fig. 6. (a) Current flow in the circuit, (b) Average PV module temperature vs time.

The input current for the current mirror circuit is therefore adjusted to 7.74 A. The DC gain (β) of the transistors, set at 75, induces a negligible decrease in the output current to 7.73 A, which substantiates the high efficiency of the current mirror design. This operational characteristic is further demonstrated by 7.

$$I_{output} = I_{input} \left(\frac{1}{1+\frac{2}{\beta^2+\beta}} \right) \tag{7}$$

The graph in Fig. 6(b) depicts the average back-surface temperature of the PV module, beginning at 25.9°C and plateauing at 33.6°C after approximately 220 seconds. This thermal stabilization, with a modest increase of 7.7°C, emphasizes the effectiveness of the hotspot mitigation without significant temperature elevation.

In comparison to traditional bypass diode techniques, the proposed method offers a more nuanced approach to managing current flow and temperature distribution across PV modules. Unlike bypass diodes, which simply shunt current around overheated cells and can lead to power losses and efficiency reduction, the current mirror circuit actively regulates current within the sub-strings. This ensures a uniform current distribution without the inefficiencies associated with diode-based bypassing. Furthermore, the slight drop in current and the subsequent stabilization of temperature as evidenced in our results underscore the viability and functionality of the current mirror circuit, setting it apart from existing mitigation techniques that may not address the subtleties of current balance and thermal regulation as effectively.

3.2 PV Module Affected by Non-Adjacent Hotspots

Fig. 7 presents a side-by-side comparison of the physical and thermal images of the second PV module subjected to analysis. This module is uniquely challenged with five non-adjacent hotspots, which are spatially distributed across its surface. Specifically, within the first sub-string, two cells exhibit elevated temperatures indicative of hotspot formation. A similar pattern is observed in the third sub-string, where an identical number of cells are similarly affected. Contrasting with the outer sub-strings, the central (second) sub-string shows a solitary hotspot. The discrete nature of these hotspots, particularly their non-adjacent positioning, could imply a pattern of stress or defect that is not uniform across the module. Such a distribution of hotspots underscores the need for a comprehensive mitigation strategy capable of addressing multiple, spatially separate areas of overheating within a single PV module.

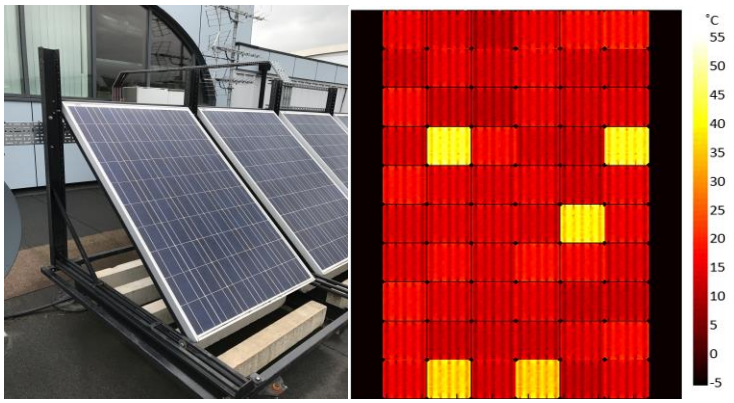

Fig. 7. Physical and thermal image of the second examined PV module affected by non-adjacent hotspots.

Fig. 8 demonstrates the thermal transition observed in the PV module during the mitigation process. Initially, the hotspots displayed temperatures ranging from 45 to 50°C, indicative of significant overheating. Upon integration with the specialized electronic device, a notable decrease in temperature was observed. Within a span of 4 minutes, the hotspots cooled down, settling into a temperature bracket of 25 to 35°C, effectively reducing the thermal stress on the affected cells and aligning their temperatures closer to those of the unimpacted areas of the module. Table 2 summarises the temperature variations of the strings over the duration of the experiment.

Table 2. Time-Resolved Thermal Analysis of PV Module Hotspots (shown in Fig. 7) Post Mitigation Circuit Implementation.

Time (min)	String 1 Avg. Temp (°C)	String 2 Avg. Temp (°C)	String 3 Avg. Temp (°C)	Overall Avg. Temp (°C)	Notes
1	50	48	50	49.3	Initial temperatures of hotspots.
2	45	43	45	44.3	Temperature begins to decrease.
3	38	36	38	37.3	Significant reduction in temperature.
4	35	33	35	34.3	Hotspots cool to near-normal levels.

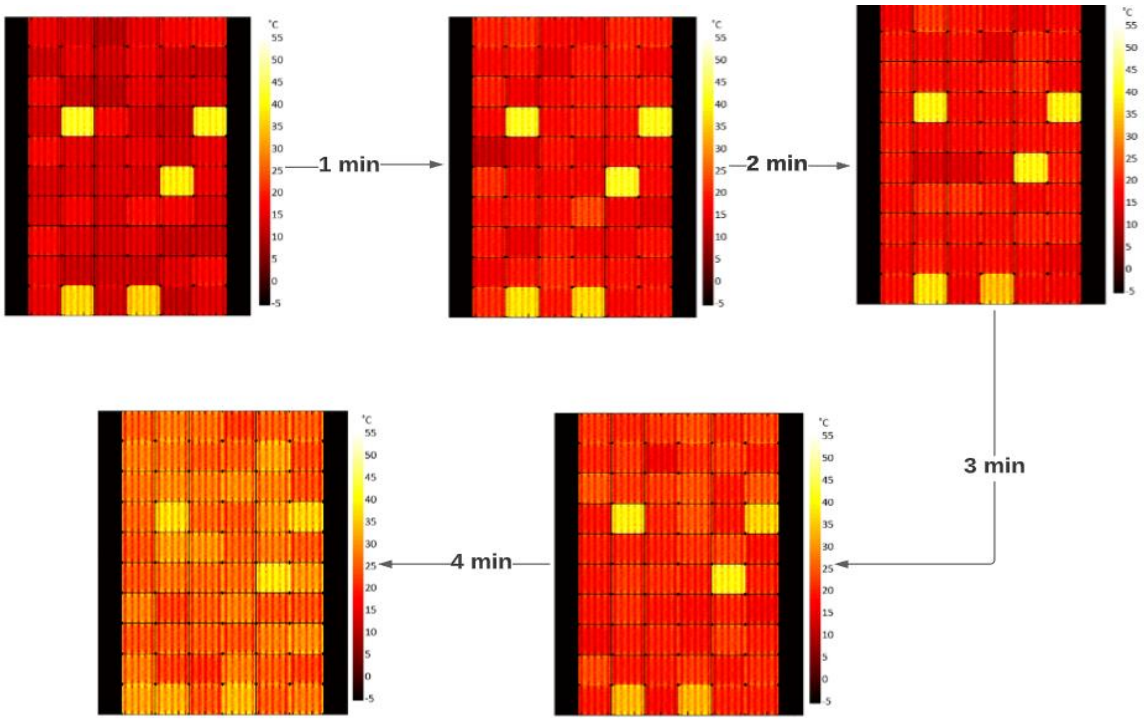

Fig. 8. Therma cycle of the PV module affected by adjacent hotspots after using the proposed circuit design.

While the implemented mitigation circuit effectively reduces hotspot temperatures, achieving parity with the temperatures of healthy solar cells remains a challenge. This discrepancy in temperature normalization can be attributed to several factors:

1) The genesis of hotspots is often linked to physical defects, such as micro-cracks within the solar cells, as documented in the literature [23-25]. Such defects intrinsically hinder thermal uniformity because they can create localized areas of increased resistance, which the mitigation circuit cannot physically rectify.
2) The circuit's design utilizes current comparators to balance the current across sub-strings, as illustrated in Fig. 3(a). This approach is effective in mitigating overcurrent conditions that exacerbate hotspots. However, it does not provide a means to fully compensate for the resultant power loss inherent to the defect sites. To achieve complete current loss identification and correction, a power electronic device would need to be installed in parallel with each solar cell. Such a solution is not practical from a cost or complexity standpoint, as it would require significant modifications to the existing PV module architecture.
3) The presence of non-uniformities despite the mitigation process suggests that the electrical characteristics of the hotspot-afflicted cells are irreversibly altered. This irreversible alteration results in a permanent deviation from the electrical characteristics of healthy cells, leading to sustained temperature differentials even after current regulation.

Fig. 9(a) depicts the measured output currents in the PV module's sub-strings. Specifically, the first sub-string's output current measures at 7.38 A, while the second and third sub-strings have outputs of 7.64 A and 7.23 A, respectively. The first current comparator, therefore, outputs the higher of the two compared currents at 7.64 A, as it surpasses the 7.38 A from the first sub-string. Similarly, the second current comparator also outputs 7.64 A, which is greater than the third sub-string's 7.23 A. A notable observation is the slight decrease in

current to 7.61 A post-comparator; this minor attenuation can be attributed to the inherent operational characteristics of the current comparators, which introduce a small voltage drop that marginally reduces the current.

The detailed current flow within the proposed mitigation circuit is captured in Fig. 9(b). Here, the current entering the current mirror is observed to be 7.61 A. The theoretical output current of the current mirror circuit is governed by 8.

$$I_{output} = I_{input} \left(\frac{1}{1+\frac{2}{\beta^2+\beta}} \right) \tag{8}$$

The temperature profile of the PV module, as illustrated in Fig. 9(c), initiates at an average of 20.8°C. Over the span of 220 seconds, or nearly 4 minutes, the module temperature exhibits a gradual ascent, stabilizing at a plateau of 29.3°C. This temperature increases of 8.5°C may suggest a correlation between the number of hotspots and the overall temperature rise within the module. Considering the steady-state temperature was achieved within the same timeframe as the previous example with fewer hotspots, the data might indicate that the circuit's ability to mitigate hotspots does not disproportionately worsen with an increase in their number.

Based on these observations, the proposed circuit demonstrates an adeptness in moderating the thermal impact of hotspots. While there is an inevitable rise in temperature associated with current regulation, the system does not precipitate an excessive increase, suggesting a balance between effective hotspot mitigation and maintaining overall module temperature within acceptable limits.

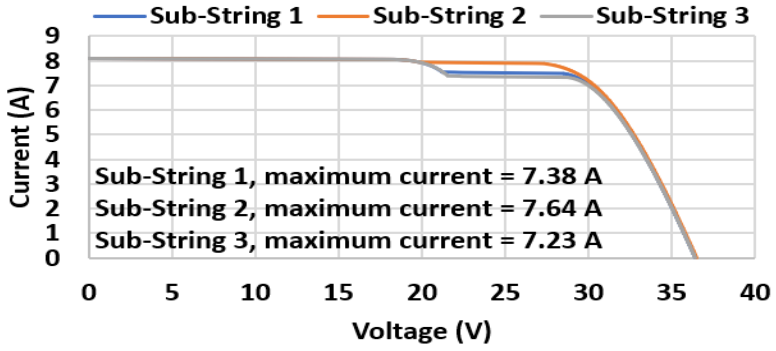

(a)

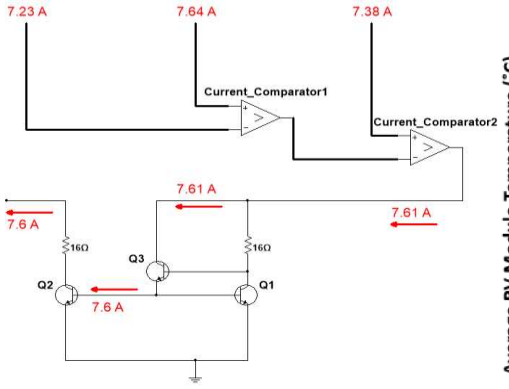

(b)

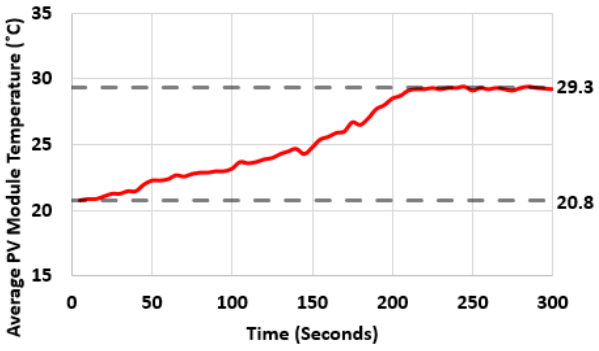

(c)

Fig. 9. (a) Output measured current in the PV sub-strings, (b) Current flow in the circuit, (c) Average PV module temperature vs time.

3.3 Output measured power

Section 3.3 evaluates the influence of our novel hotspot mitigation technique on the power output of two distinct PV modules. Prior to and following the integration of the mitigation device, each module underwent a series of tests under Standard Test Conditions (STC) to ascertain any variations in performance. These tests were conducted using a state-of-the-art PV simulator (SPI-Sun Simulator 4600SLP), and the power-voltage (P-V) curves were meticulously recorded via a LabVIEW software interface. Throughout the testing procedure, both the temperature and irradiance were meticulously controlled, maintained at approximately 25°C and 1000 W/m^2, respectively, to ensure consistency with STC parameters.

The resulting P-V curves, as depicted in Fig. 10, provide a comparative analysis of the modules' performance. For the first PV module, shown in Fig. 10(a), which suffered from the thermal effects of three adjacent hotspots, there was a discernible increase in maximum power output from 211.9 W to 218.2 W after the mitigation device was implemented. This improvement represents a noteworthy efficiency gain of approximately 3%. Similarly, the second PV module, characterized by non-adjacent hotspots and illustrated in Fig. 10(b), demonstrated a more substantial increase in performance, with power output rising from 203.7 W to 214.6 W, translating to an efficiency enhancement of 5.35%.

These increments in power output underscore the effectiveness of the mitigation device not only in reducing the temperature of hotspot-affected cells but also in enhancing the overall energy production of the PV modules. The differential in performance uplift between modules affected by adjacent and non-adjacent hotspots further suggests that the mitigation technique may have a variable impact depending on the spatial distribution of the hotspots within the module array.

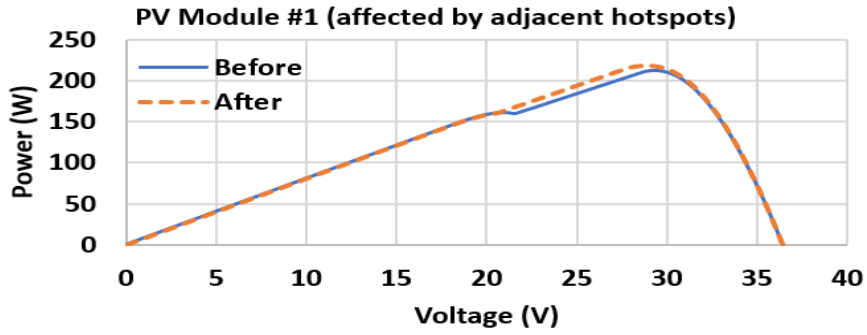

(a)

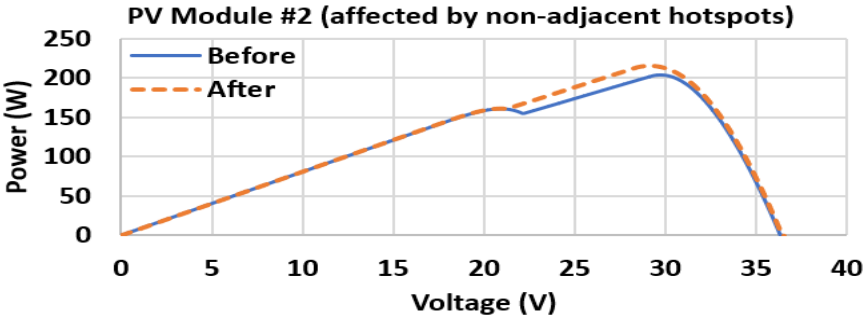

(b)

Fig. 10. Output measured P-V curve at STC condition, (a) PV module affected by adjacent hotspots, shown in Fig. 4, (b) PV module affected by non-adjacent hotspots, shown in Fig. 7.

3.4 Thermal sensitivity and cost-effectiveness of the proposed electronic device

The novel circuit introduced in this study is designed to function autonomously, powered directly by the output current from the PV module, thus negating the need for an external power supply. This design choice significantly reduces the circuit's power consumption to a mere 10 mW. This efficiency is achieved by two mechanisms: firstly, the circuit does not employ pulse width modulation (PWM) for the Bipolar Junction Transistors (BJTs), thereby saving energy; secondly, the BJTs and current comparators act as the primary active components, creating an alternate route for current flow without necessitating any direct current (DC) to DC power conversion. Cost considerations are paramount in the deployment of any new technology. The circuit's affordability is ensured through the use of inexpensive components, each costing less than a dollar, summing up to a minimal total expense. The circuit is composed of merely two current comparators and two NPN transistors, circumventing the need for bypass diodes, which adds to the cost-saving aspect.

The circuit's reliance on passive components ensures that the inherent efficiency of the PV module is preserved without interference. However, thermal sensitivity of the BJTs is an important consideration. Elevated temperatures can impede the switching functionality of BJTs [26, 27]. It is, therefore, imperative to select NPN transistors that are rated for higher operational temperatures, ideally exceeding 90°C.

To ascertain the circuit's performance under thermal duress, an experimental setup was employed where the input pins were subjected to a high current load of 100 A. The resulting thermal profile, as captured in Fig. 11(a), shows that the circuit's pin connections reached a high but manageable temperature of 90°C. Concurrently, Fig. 11(b) illustrates the thermal state of the NPN transistors, which maintained a maximum temperature of 52°C. The absence of critical overheating in these components confirms the circuit's reliability across a spectrum of temperature conditions, rendering it a viable solution for diverse PV applications, from small-scale residential systems to expansive commercial installations.

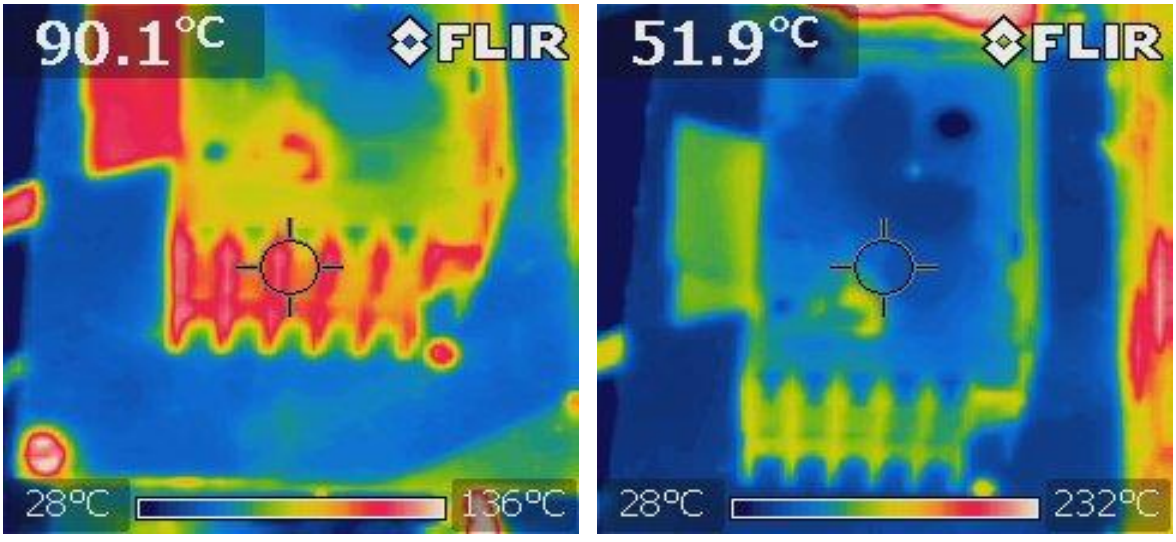

(a) (b)

Fig. 11. (a) Thermal image taken for the input pins of the circuit, (b) Thermal image taken for the actual NPN Transistors of the circuit.

4. Conclusions

The escalating demand for renewable energy solutions has amplified the focus on the reliability and efficiency of PV systems. In this context, the challenge of hotspot mitigation within PV modules has emerged as a critical area of research and development. This paper presented a novel electronic circuit designed to address the pervasive issue of hotspots in PV modules, which are known to precipitate efficiency losses and potentially hazardous operating conditions. Our proposed circuit, characterized by its simplicity and effectiveness, operates autonomously, leveraging the output current of the PV module itself. The absence of an external power supply and the circuit's minimal power consumption represent significant strides towards energy efficiency and sustainability. Moreover, the cost-effectiveness of the circuit is evident in its reliance on low-cost components—two current comparators and two NPN transistors—thereby presenting an economically viable alternative to more complex and expensive hotspot mitigation technologies.

Thermally, the circuit has demonstrated resilience. The experimental validation, which involved subjecting the circuit to high current loads, confirmed its thermal stability, with component temperatures remaining within safe operating limits. This robust performance indicates the circuit's suitability for a broad range of PV installations, from small-scale residential to large-scale industrial applications.

Performance-wise, the circuit has shown a marked increase in the output power of PV modules post-integration, with improvements of approximately 3% and 5.35% for modules affected by adjacent and non-adjacent hotspots, respectively. These gains underscore the dual benefit of the proposed design—it not only mitigates the thermal issues associated with hotspots but also enhances the overall power output of the PV modules.

It is also crucial to acknowledge the limitations encountered. While the circuit significantly reduced hotspot temperatures, bringing them closer to those of healthy cells, it did not entirely normalize them. The enduring non-uniformities could be attributed to the irreversible physical changes within the cells caused by defects such as micro-cracks. Furthermore, while the circuit facilitated a more uniform distribution of current, it was not designed to correct the power losses at the site of defects.

Looking forward, the insights garnered from this research could spur further innovations in PV module design and hotspot mitigation techniques. Continuous advancements in material science and electronics may soon enable the integration of self-healing materials or more advanced electronic components that could automatically adjust to changing thermal conditions, thereby further elevating the reliability and longevity of PV modules.

In summary, this research contributes a practical solution to a significant challenge in the field of solar energy. The proposed circuit not only offers a new dimension in thermal management within PV modules but also represents a leap towards more resilient and economically feasible renewable energy technologies. The implications of this work extend beyond immediate performance enhancements, promising a future where the robust integration of solar energy into the global energy mix is not only possible but also pragmatically attainable.

Acknowledgement

Sandia National Laboratories is a multimission laboratory managed and operated by National Technology & Engineering Solutions of Sandia, LLC, a wholly owned subsidiary of Honeywell International Inc., for the U.S. Department of Energy's National Nuclear Security Administration under contract DE-NA0003525. This article describes objective technical results and analysis. Any subjective views or opinions that might be expressed in this article do not necessarily represent the views of the U.S. Department of Energy or the Unites States Government.

References

[1] Yin, O. W., & Babu, B. C. (2018). Simple and easy approach for mathematical analysis of photovoltaic (PV) module under normal and partial shading conditions. Optik, 169, 48-61.

[2] Chantana, J., Kawano, Y., Kamei, A., & Minemoto, T. (2019). Description of degradation of output performance for photovoltaic modules by multiple regression analysis based on environmental factors. Optik, 179, 1063-1070.

[3] Yang, Z., Liao, K., Chen, J., Xia, L., & Luo, X. (2021). Output performance analysis and power optimization of different configurations half-cell modules under partial shading. Optik, 232, 166499.

[4] Guerriero, P., & Daliento, S. (2019). Toward a hot spot free PV module. IEEE Journal of Photovoltaics, 9(3), 796-802.

[5] Livera, A., Theristis, M., Makrides, G., & Georghiou, G. E. (2019). Recent advances in failure diagnosis techniques based on performance data analysis for grid-connected photovoltaic systems. Renewable energy, 133, 126-143.

[6] Tang, S., Xing, Y., Chen, L., Song, X., & Yao, F. (2021). Review and a novel strategy for mitigating hot spot of PV panels. Solar Energy, 214, 51-61.

[7] Dhimish, M., Mather, P., & Holmes, V. (2018). Evaluating power loss and performance ratio of hot-spotted photovoltaic modules. IEEE Transactions on Electron Devices, 65(12), 5419-5427.

[8] Cheng, T., Al-Soeidat, M., Lu, D. D. C., & Agelidis, V. G. (2019). Experimental study of PV strings affected by cracks. The Journal of Engineering, 2019(18), 5124-5128.

[9] Dhimish, M., Holmes, V., Mehrdadi, B., & Dales, M. (2017). The impact of cracks on photovoltaic power performance. Journal of Science: Advanced Materials and Devices, 2(2), 199-209.

[10] Satpathy, P. R., Sharma, R., Panigrahi, S. K., & Panda, S. (2020, July). Bypass diodes configurations for mismatch and hotspot reduction in PV modules. In 2020 International Conference on Computational Intelligence for Smart Power System and Sustainable Energy (CISPSSE) (pp. 1-6). IEEE.

[11] Shin, W. G., Jung, T. H., Go, S. H., Ju, Y. C., Chang, H. S., & Kang, G. H. (2015). Analysis on thermal & electrical characteristics variation of PV module with damaged bypass diodes. Journal of the Korean Solar Energy Society, 35(4), 67-75.

[12] Ahmad, F. F., Ghenai, C., Hamid, A. K., Rejeb, O., & Bettayeb, M. (2021). Performance enhancement and infra-red (IR) thermography of solar photovoltaic panel using back cooling from the waste air of building centralized air conditioning system. Case Studies in Thermal Engineering, 24, 100840.

[13] Ali, M. U., Saleem, S., Masood, H., Kallu, K. D., Masud, M., Alvi, M. J., & Zafar, A. (2022). Early hotspot detection in photovoltaic modules using color image descriptors: An infrared thermography study. International Journal of Energy Research, 46(2), 774-785.

[14] Manno, D., Cipriani, G., Ciulla, G., Di Dio, V., Guarino, S., & Brano, V. L. (2021). Deep learning strategies for automatic fault diagnosis in photovoltaic systems by thermographic images. Energy Conversion and Management, 241, 114315.

[15] Berghout, T., Benbouzid, M., Bentrcia, T., Ma, X., Djurović, S., & Mouss, L. H. (2021). Machine Learning-Based Condition Monitoring for PV Systems: State of the Art and Future Prospects. Energies, 14(19), 6316.

[16] Dhimish, M., Holmes, V., Mather, P., & Sibley, M. (2018). Novel hot spot mitigation technique to enhance photovoltaic solar panels output power performance. Solar Energy Materials and Solar Cells, 179, 72-79.

[17] Ghosh, S., Yadav, V. K., & Mukherjee, V. (2020). A novel hot spot mitigation circuit for improved reliability of PV module. IEEE Transactions on device and materials reliability, 20(1), 191-198.

[18] Dhimish, M., & Tyrrell, A. M. (2022). Power loss and hotspot analysis for photovoltaic modules affected by potential induced degradation. npj Materials Degradation, 6(1), 1-8.

[19] d'Alessandro, V., Guerriero, P., & Daliento, S. (2013). A simple bipolar transistor-based bypass approach for photovoltaic modules. IEEE Journal of Photovoltaics, 4(1), 405-413.

[20] Tang, S., Xing, Y., Chen, L., Song, X., & Yao, F. (2019). Review and a novel strategy for mitigating hot spot of PV panels. Solar Energy, 214, 51-61.

[21] Ghosh, S., Yadav, V. K., & Mukherjee, V. (2020). A novel hot spot mitigation circuit for improved reliability of PV module. IEEE Transactions on Device and Materials Reliability, 20(1), 191-198.

[22] Al Tarabsheh, A., Abughali, A. M., AlSalmani, A. M., AlSoufi, A. J., & Baba, L. B. (2023). Programmable photovoltaic submodules for hotspot mitigation. International Journal of Sustainable Engineering, 16(1), 1-13.

[21] Ayache, K., Chandra, A., & Chériti, A. (2019). An embedded reconfiguration for reliability enhancement of photovoltaic shaded panels against hot spots. IEEE Transactions on Industry Applications, 56(2), 1815-1826.

[22] Jordan, D. C., Silverman, T. J., Sekulic, B., & Kurtz, S. R. (2017). PV degradation curves: non-linearities and failure modes. Progress in Photovoltaics: Research and Applications, 25(7), 583-591.

[23] Dhimish, M., & Lazaridis, P. I. (2021). An empirical investigation on the correlation between solar cell cracks and hotspots. Scientific reports, 11(1), 1-11.

[24] Zhao, Z., Jiang, N., Ma, Z., & Qin, G. (2018). Impact of finger numbers on the performance of proton-radiated SiGe power HBTs at room and cryogenic temperatures. Microelectronics Reliability, 91, 194-200.

[25] Petrov, A.S., Tapero, K.I., Galimov, A.M. and Zebrev, G.I., 2019. Degradation of bipolar transistors at high doses obtained at elevated temperature applied during gamma-irradiation. Microelectronics Reliability, 100, p.113378.

[26] Dhimish, M., 2019. 70% decrease of hot-spotted photovoltaic modules output power loss using novel MPPT algorithm. IEEE Transactions on Circuits and Systems II: Express Briefs, 66(12), pp.2027-2031.

[27] Khodapanah, M., Ghanbari, T., Moshksar, E. and Hosseini, Z., 2023. Partial shading detection and hotspot prediction in photovoltaic systems based on numerical differentiation and integration of the P− V curves. IET Renewable Power Generation, 17(2), pp.279-295.